6-2013

Design and Construction of an Optical Tweezers

Pavel Aprelev
Union College - Schenectady, NY

Design and Construction of an Optical Tweezers.

By:

Pavel Aprelev

Advisor:

Chad Orzel

****

Submitted in partial fulfillment
of the requirements for
Honors in the Department of Physics and Astronomy

UNOIN COLLEGE

June, 2013

ABSTRACT

APRELEV, PAVEL Design and Construction of an Optical Tweezers.

Department of Physics and Astronomy, June 2013.

ADVISOR: Chad Orzel

We constructed an optical tweezers apparatus, used it to trap transparent micron-sized particles, and moved those particles within a sample by moving the sample relative to the focal point of the trapping beam. The optical trap was based on the fact that focused coherent light creates forces on dielectric objects that point towards the focal point. The magnitude and the span of the force are dependent on the size of the focal point of the beam - generally around 1μm - and the intensity of light. We used an 808 nm 200 mW laser and a piezoelectric stage to trap 1μm plastic beads and move them in 3D. Using a LabView program, we were able to move the stage at precise speeds and thus determine the forces within the focal point of the beam for different powers of the laser. We measured forces as large as 0.5 pN for a laser beam power of 80 mW.

Contents

Chapter 1

Introduction

Reference 1, by Keir C. Neuman and Steven M. Block, provides an excellent overview of history and operation of optical tweezers.

Optical tweezers use a focused laser beam in order to trap transparent micron-sized particles at the focal point. The trapping force appears as a result of refracting light that goes through the particle, resulting in forces that push the particle towards the center of the focus of the beam.

1.1 History

In early 1970s, Arthur Ashkin pioneered the field of optical trapping by demonstrating that optical forces could displace micron-sized dielectric particles in both water and air.[2] He stably trapped particles by designing a three-dimensional trap that relied on two laser beams that focused at the same point from different directions.[3] Developing the system further, he achieved trapping using only one laser. The trap was based on the force due to the gradient of the beam.[4] The single laser optical trapping system became known as "optical tweezers."[5] Ashkin and his team used it extensively in experiments that dealt with manipulating live bacteria and viruses.[6]

Optical tweezers are able to apply forces on the scale of pico-Newtons on micron-sized particles without any physical contact. Moreover, the trapped objects can be moved by very precise distances with nanometer resolution. As a result, optical tweezers are widely used in the study of molecular motors[7], colloids[8], and polymers[9]. Much of the recent progress in optical

trapping has been made possible by recent technological developments. The commercially available three-dimensional piezoelectric stages, for example, contributed to unprecedented control of the trapped particles and led to better calibration of the forces and displacements in the traps. Moreover, high-bandwidth position detectors help improve force calibration for very stiff traps and extend the detection bandwidth of optical trapping measurements.[10] At the same time, recent theoretical work has led to better methods of calculation of optical forces on spherical objects of different sizes.[11]

1.2 Theory

An optical trap is created by focusing a laser beam into a point. A dielectric particle near the focal point will experience forces that will push it towards the center. The forces are results of three basic laws of physics: the fact that photons carry momentum[A]; the momentum principle – equation (1) below; and Newton's third law – equation (2) below:

$$\vec{F}_{net} = \frac{d\vec{p}}{dt} \quad (1)$$

$$\vec{F}_{1,2} = \vec{F}_{2,1} \quad (2)$$

There are two forces that act on the bead at the same time: (1) a force due to the scattering of the photon from the surface and (2) a force due to the refraction of the photon as it enters and leaves the bead. The scattering force points in the direction of the beam but is smaller than the refraction forces (about 30% at the trapping point).[11] The refraction forces are easier to see when the force vector is broken down into two components: the horizontal force

[A] Even though the quantum view of light is not used to describe the operation of optical tweezers, the principle is easier to visualize when thinking about light in terms of particles rather than waves.

that brings the bead to the center of the beam, and the vertical force that brings the bead into the focal plane.

Figure 1A below illustrates the basis behind the horizontal forces in the trap. The photons that approach the bead from the right get refracted to the left upon entering the bead and again upon leaving the bead due to the difference of the indices of refraction between the medium and the particle. The refraction results in a change of momentum of the photons to the left and thus a force on the bead to the right. Similarly, the photons that approach the bead from the right get refracted to the right upon entering the bead and again upon leaving the bead. The refraction results in a change of momentum of the photons to the right and thus a force on the bead to the left. The bead is, thus, pushed in the direction of higher light intensity.

Figure 1B below illustrates the basis behind the vertical forces in the trap. The photons that approach the bead from the left get refracted to the left upon entering the bead and again upon leaving the bead. The refraction results in a change of momentum of the photons to the bottom-left and thus a force on the bead to the top-right. The photons that approach the bead from the right get refracted to the right upon entering the bead and again upon leaving the bead. The refraction results in a change of momentum of the photons to the bottom-right and thus a force on the bead to the top-left. The sum of the forces is up toward the focal point. The bead is thus pushed towards the focal point. The forces are explained in Figure 1.B below

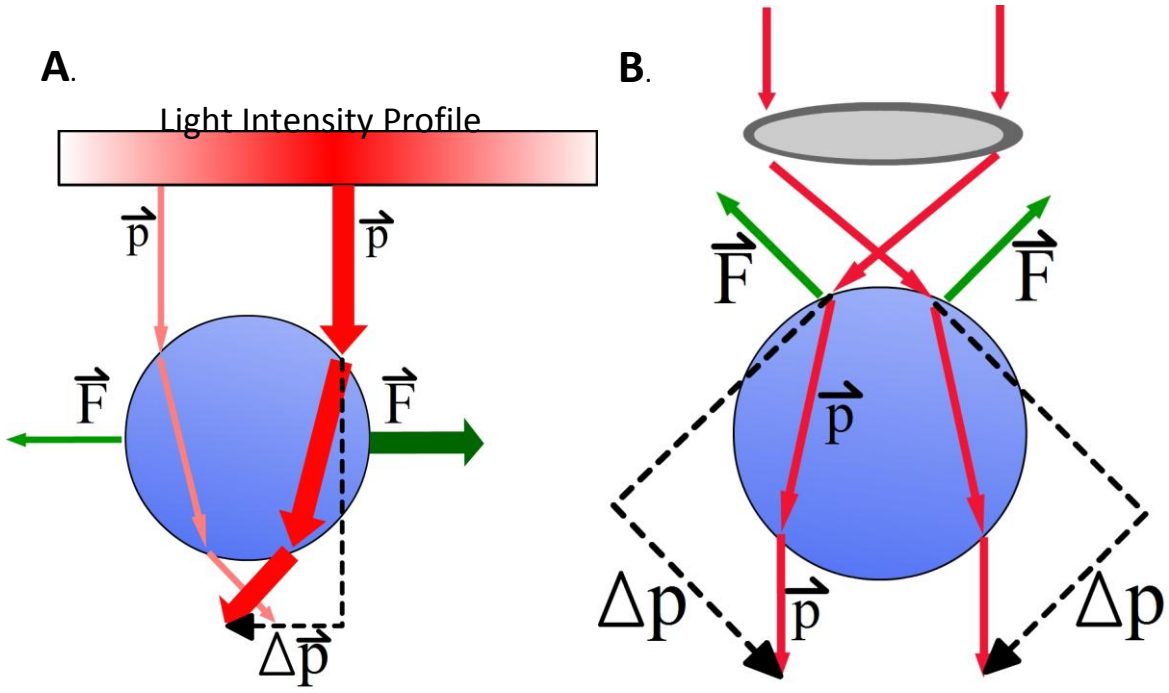

Figure 1. Ray optics description of the gradient force. Image (A) shows how beads are trapped in the horizontal direction. Red arrows represent the photons. The brighter the red and the thicker the arrow, the more photons are represented. The photons that approach the bead from the right get refracted to the left upon entering the bead and again upon leaving the bead. The refraction results in a change of momentum of the photons to the left and thus a force on the bead to the right. Similarly, the photons that approach the bead from the right get refracted to the right upon entering the bead and again upon leaving the bead. The refraction results in a change of momentum of the photons to the right and thus a force on the bead to the left. Since the force to the right is stronger than the force to the left, the bead would move to the right until the forces on both sides become equal that is until the bead is in the middle of the beam. Image (B) shows how beads are trapped in the vertical direction. The photons that approach the bead from the left get refracted to the left upon entering the bead and again upon leaving the bead. The refraction results in a change of momentum of the photons to the bottom-left and thus a force on the bead to the top-right. The photons that approach the bead from the right get refracted to the right upon entering the bead and again upon leaving the bead. The refraction results in a change of momentum of the photons to the bottom-right and thus a force on the bead to the top-left. The sum of the forces is up toward the focal point. The bead, thus, moves to the focal point. If the bead starts above the focal point, similar processes push the bead towards the focal point.

As a result, the bead is kept in the focal point of the trap. The diagram to scale is presented in Figure 2 below.

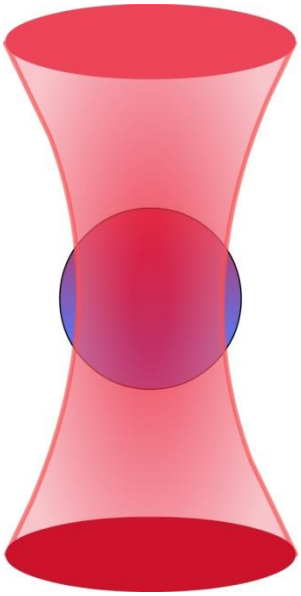

Figure 2. A diagram of a bead in a trap to scale. The light does not focus into a point, but creates a Gaussian distribution of intensity around the beam waist. Nevertheless, the processes explained in Figure 1 still work as described. Because of the scattering force, however, the bead is a little lower than the waist of the beam.

In order to calibrate the force of the trap, we took advantage of the fact that the trapped particles were in water. Moving particles with size of the order of microns in a liquid with speeds of approximately 10 microns/second experience a drag force that is proportional to the velocity and can be described by equation (3) below:

$$F_{drag} = 6\pi\eta Rv \qquad (3)$$

where F_{drag} is the force of drag on the particle due to the surrounding liquid, η is the viscosity of the liquid, R is the radius of the particle, and v is the velocity of the particle relative to the

medium.[12] Since η for water is known ($1.002*10^{-3}$ N s/m^2 at 20^o C) and the radius of the beads is known ($0.5*10^{-6}$ m), we can relate the velocity of the particle to the force of drag on it.

Since moving particles in water experience a drag force that is proportional to their velocity, we can slowly increase the velocity until the particle falls out of the trap. At that instant, the force due to the laser and the force due to the drag will be equal. Thus, we can move the trapped particle relative to the medium with precise speeds and see which speeds are associated with the particle falling out of the trap.

Chapter 2

Experimental Setup

During the course of the project, we attempted two different set-ups: one using a 200 mW infrared laser diode (Sanyo DL-8141) and the other using a fiber-coupled 2-watt infrared laser (Lasertel LT-2010-01-1708) as the source of light. The first design was successful, so it will be described first in section A. The second setup ended up not working, so its shortcoming will be discussed in section B.

2.1 Sanyo DL-8141 Design.

The setup consists of a 200 mW infrared laser diode (Sanyo DL-8141), a telescope, an objective, a Thorlabs Piezo controlled stage (MDT963A), a camera, and stirring mirrors. We aligned the optics such that the beam would be coaxial with the objective and occupy approximately half of the front aperture to allow for fine adjustments of the position of the beam. The schematic of the apparatus is presented below in Figure 3.

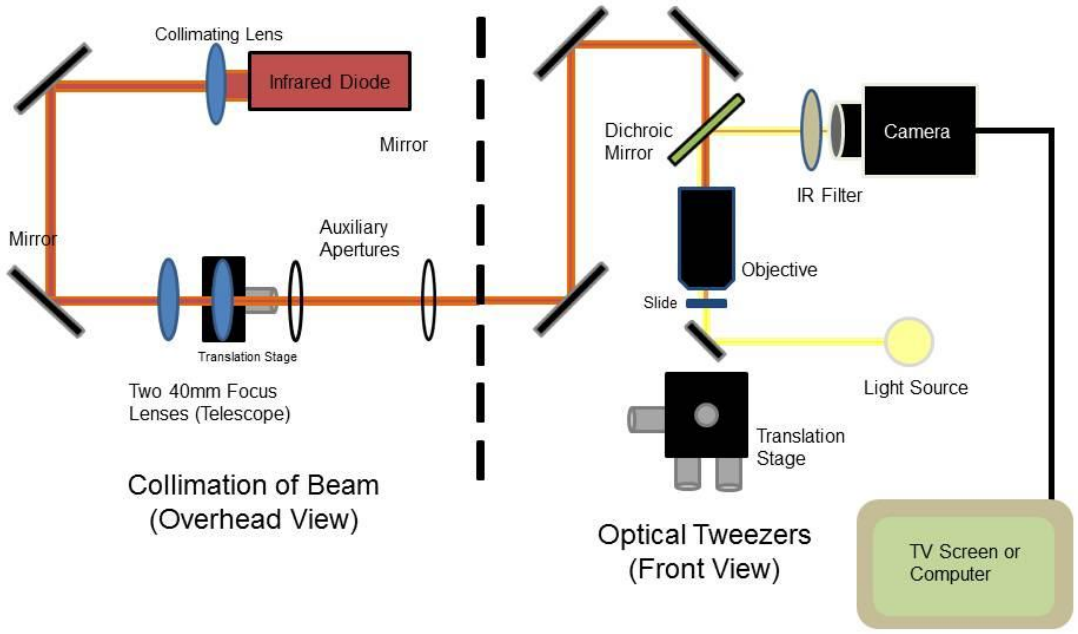

Figure 3. Schematic of the apparatus. The beam exits the laser, gets collimated by the collimating lens, and gets steered by two mirrors into the telescope. The telescope performs fine adjustments of the collimation of the beam needed for correct focal point at the objective. The beam then passes the auxiliary apertures and gets steered into through the dichroic mirror into a 100x objective, where it gets focused on the slide with plastic beads to perform trapping. The slide is illuminated from the bottom to allow viewing of the slide with the camera. The translation stage is connected to a driver, which is in turn connected to a computer via a serial cable.

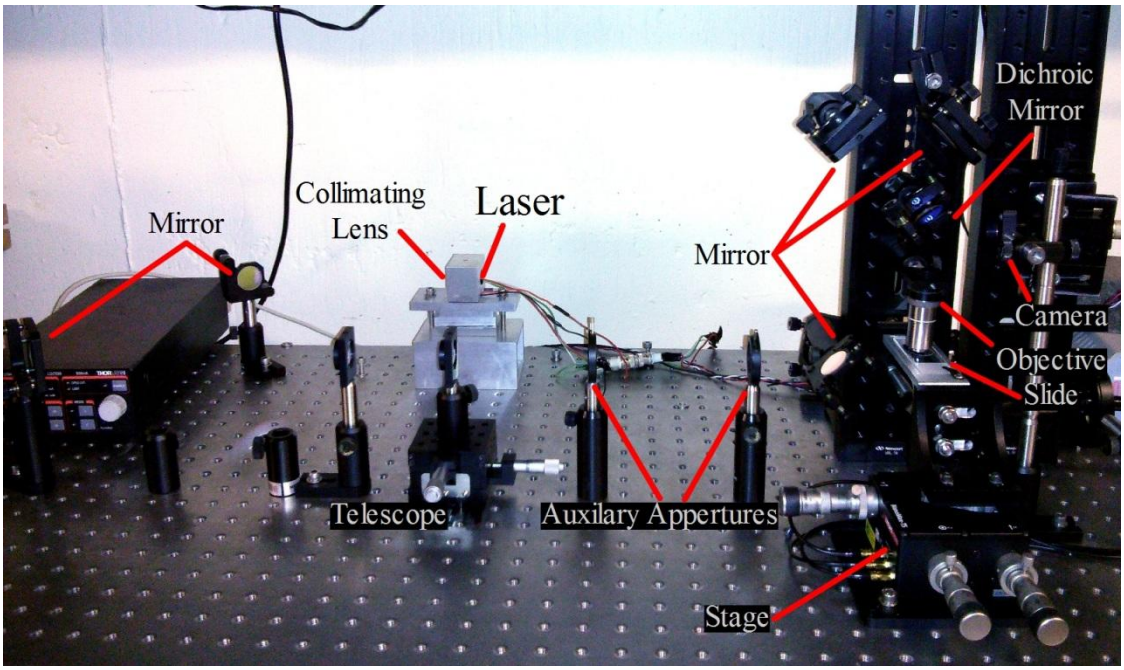

Figure 4. A labeled photograph of the apparatus. For a description of components, see Fig. 3.

2.1.1 Laser

We picked the 200 mW infrared diode laser (Sanyo DL-8141) for its relatively low cost, 808nm wavelength, and appropriate power. Diode lasers do not output a collimated beam so they require a separate collimation lens. In our setup, the collimation lens was a part of the collimation tube (ThorLabs LT230A) and was integrated into the laser mount. The lens is able to provide crude collimation, but finer adjustments are performed with a telescope discussed below. In order to keep the power output of the laser constant, we used a ThorLabs laser diode controller (ThorLabs LDC 500). The beam was faintly visible to the naked eye, but IR fluorescent cards, an IR viewer, and a cell-phone camera helped tremendously with alignment of the beam.

Prior to measuring the forces associated with our setup, we measured the dependency of our laser's power on the current supplied to the laser diode. The relationship is presented

below in Figure 5. It can be seen that the relationship is linear for currents between 50 and 75 mA, but at higher currents the power yield level off at approximately 160 mW.

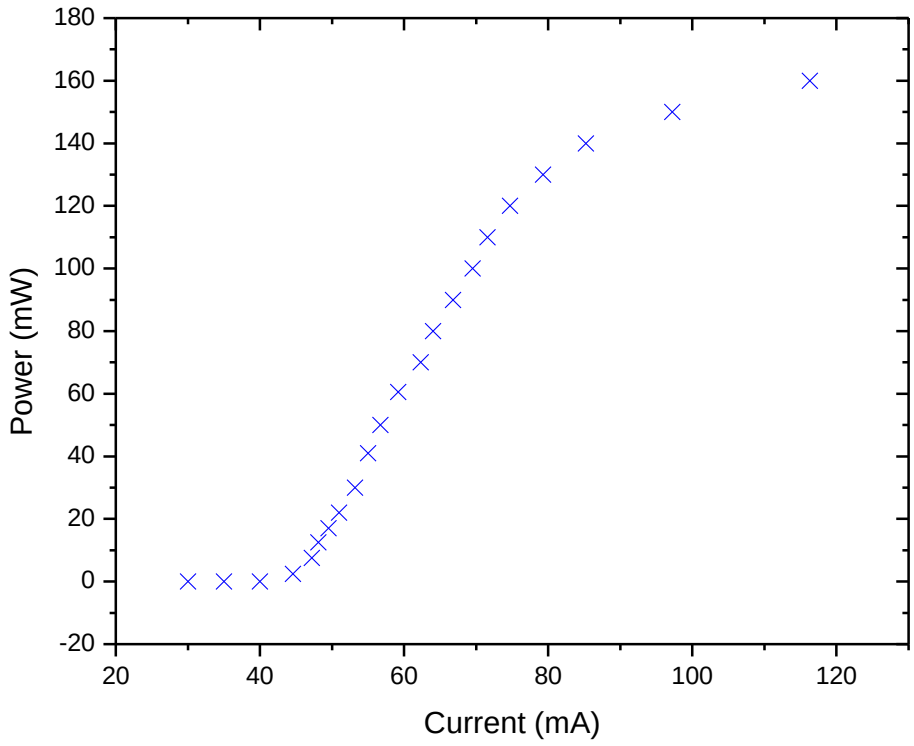

Figure 5. The relationship between laser output power and current supplied to the laser diode.

2.1.2 Collimation Telescope

The telescope consists of two identical lenses, positioned approximately two focal distance apart. Thus, by moving the second lens, we are able to finely adjust the collimation of the exiting beam. The collimation is important for optical tweezers, because we want to trap the particle exactly at the focal point, so that we can see it.

With an optical microscope, you can only see the plane that is perpendicular to the objective and is a focal distance away. Thus, in order to see the bead with an optical microscope, it must be located at the focal plane. That is only possible if the beam that is going into the objective is perfectly collimated. If the incoming beam is converging, it focuses closer to the objective than the viewing plane. If the incoming beam is diverging, it focuses further away from the objective than the viewing plane. In both cases, the particle would still get trapped, but it would be impossible to see it. The illustration of importance of collimation of the beam is presented in Figure 6 below.

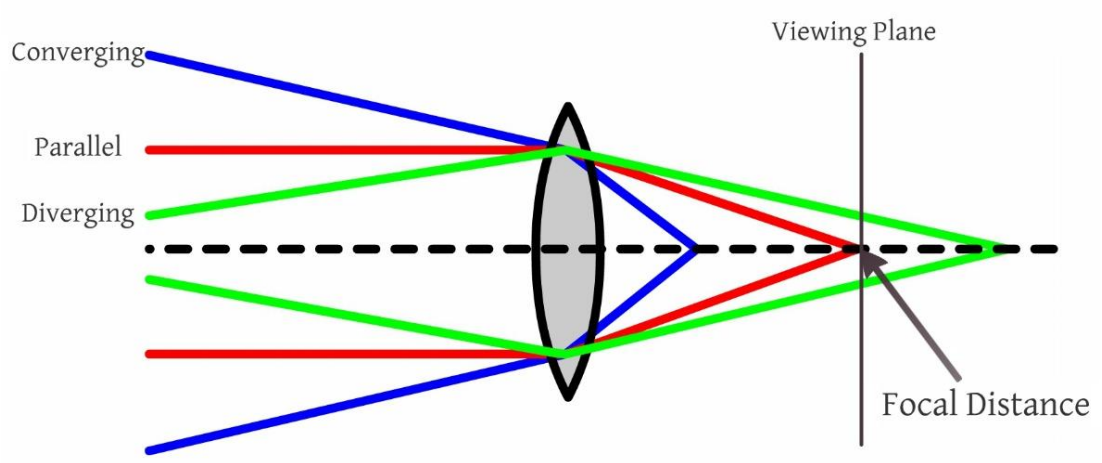

Figure 6. Importance of Collimation. In order to see an object with an optical microscope, it must be at the viewing plane, which is perpendicular to the objective and goes through the focal distance point. That is only possible if the beam that is going into the objective is perfectly collimated. If the incoming beam is converging, it focuses closer to the objective than the viewing plane. If the incoming beam is diverging, it focuses further away from the objective than the viewing plane. In both cases, the particle would still get trapped, but it would be impossible to see.

2.1.3. Dichroic Mirror

The dichroic mirror lets through infrared light and reflects visible light. Thus, the laser goes through it unaffected and the visible image from the objective is reflected into the camera. (See Fig. 3)

2.1.4 Microscope Objective

In order to trap particles effectively, it is necessary to have a high gradient of intensity and thus use a high-magnification microscope objective. We used a 100x objective, but it is possible to use lower magnification objectives. With a 100x objective the focal point is very close to the objective, leading to direct contact between the objective and the slide, which contains the bead. The direct contact causes micro-currents in the slide, and thus adds undesired forces. This also means that you can only trap beads closely to the cover slip. Thus, in the future, we might try using a smaller magnification objective in order to increase the z-axis range of trapping and eliminate micro-currents that are caused by direct contact of the objective and slide. There are 100x objectives with much higher working distances available on the market, but they are generally more expensive.

For a more detailed discussion of the micro-currents, see section 5.1 of the discussion.

2.1.5 Piezo-controlled stage.

In order to find particles to trap and effectively control the trapped particles, we used a translation stage that had 3 axes of motion. The translation stage could be controlled manually with micron-scale knobs and remotely with piezoelectrics. The piezoelectrics have a range of 40 microns and a maximum operating voltage of 75V, which is supplied by a power supply. The relationship between the applied voltage and the displacement is presented in Figure 7 below.

The power supply can be connected to a computer via a serial port. We wrote a program in LabView that sends signals with coordinates to the serial port controller of the computer, thus moving the stage at very precise velocities. The LabView program is explained in detail in the procedure section below.

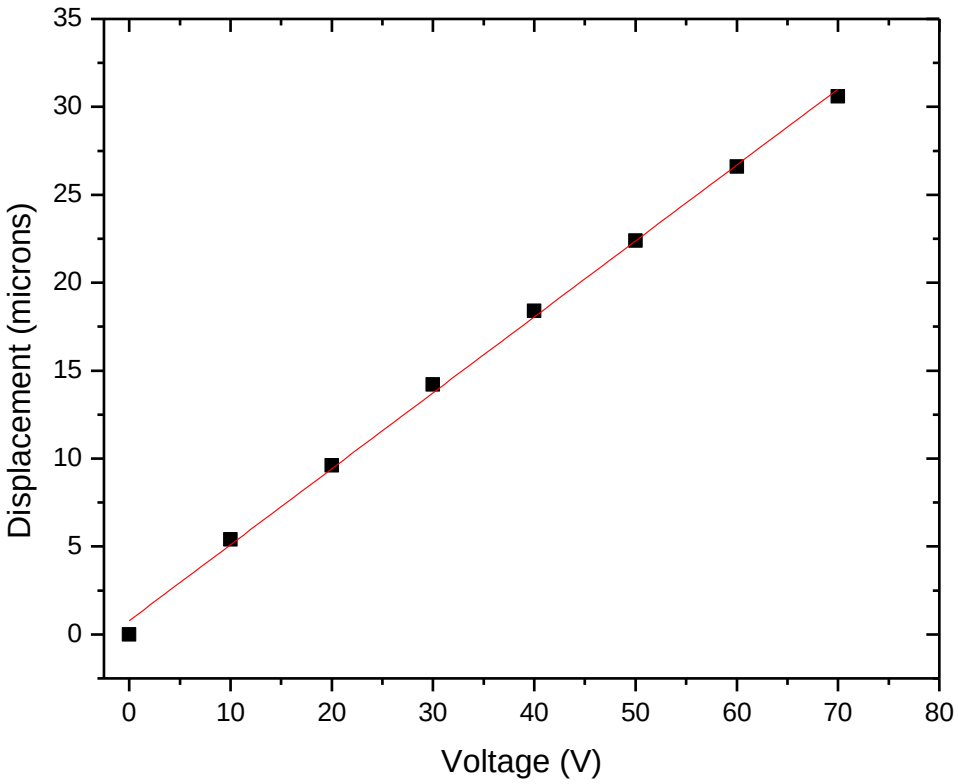

Figure 7. Plot of Stage displacement vs. voltage on the piezoelectics.

2.1.6 Slide Samples

The slide samples consisted of a glass slide and a cover slip freely resting on top of it. Since the slide was positioned horizontally on the stage, it relied on friction and a spring on a screw to keep in place. The cover was held in place only by the surface tension of the water in the sample. This allowed us to quickly create the slides as it required very little preparation. We had to be careful when creating the samples, however, because too much solution would cause the cover slip to freely drift on top of the side.

2.1.7 CCD Camera

The CCD Camera was attached to a monitor, which allowed us to see the slide in real time. The camera had an IR filter in front of it in order to eliminate the scattered laser light from the image.

2.2 Fiber-Coupled 2-Watt Infrared Laser (Lasertel LT-2010-01-1708) Design

We attempted to achieve trapping by used a fiber-coupled 2-watt infrared laser (Lasertel LT-2010-01-1708) as the source of light. The advantages of the design included price ($100 for laser) and convenience (multimode fiber output allowed to make the setup much more compact). It was impossible, however, to achieve trapping with the unfiltered beam, as it was very non-Gaussian and thus did not focus into a point. The comparison of an unfiltered Lasertel beam with a Sanyo beam is presented in Figure 8 below.

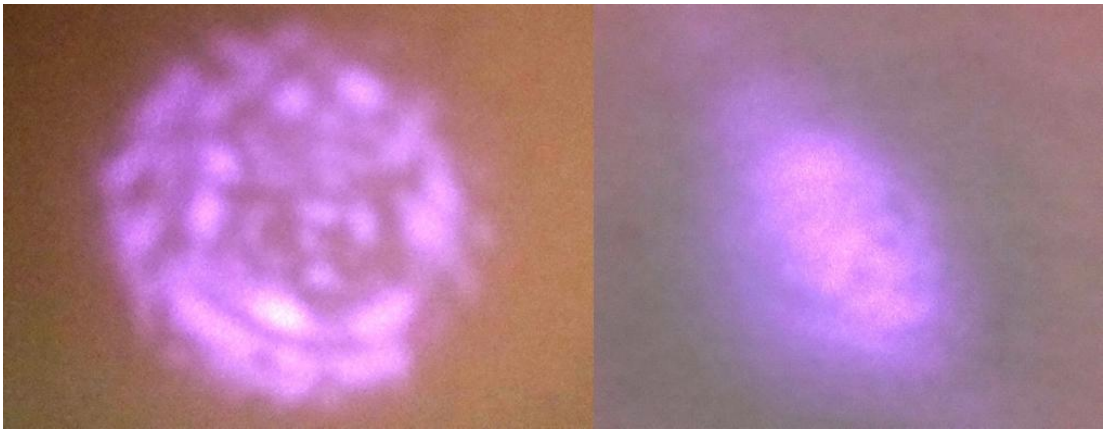

Figure 8. An unfiltered beam of a fiber-coupled Lasertel LT-2010-01-1708 laser (top left) and an unfiltered beam of the Sanyo DL-8141 diode laser for comparison. We obtained these pictures by expanding the beams with a lens, projecting them on a sheet of white paper, and photographing them with a simple cellphone camera. The cellphone camera did not have an IR filter on it, so it could detect IR light.

We attempted to filter the beam using multi-to-single mode fiber coupling as well as using a spatial filter. The setups for both methods are presented in Figures 9 and 10 respectively.

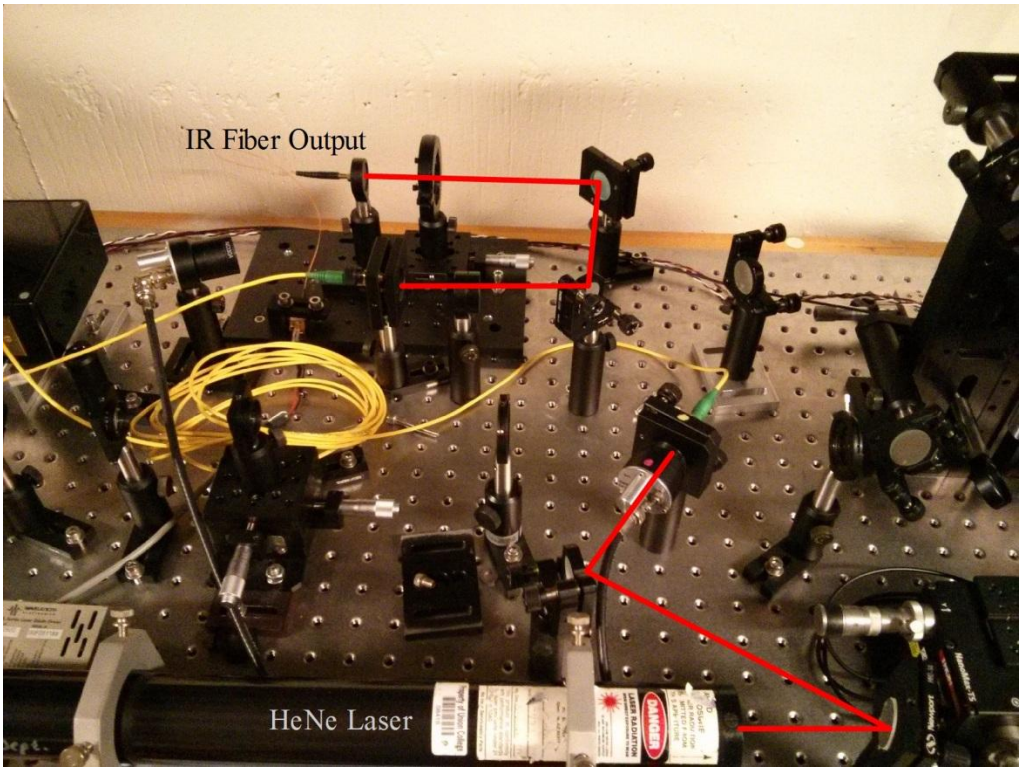

Figure 9. The setup for a single mode optical fiber filtration of the beam.

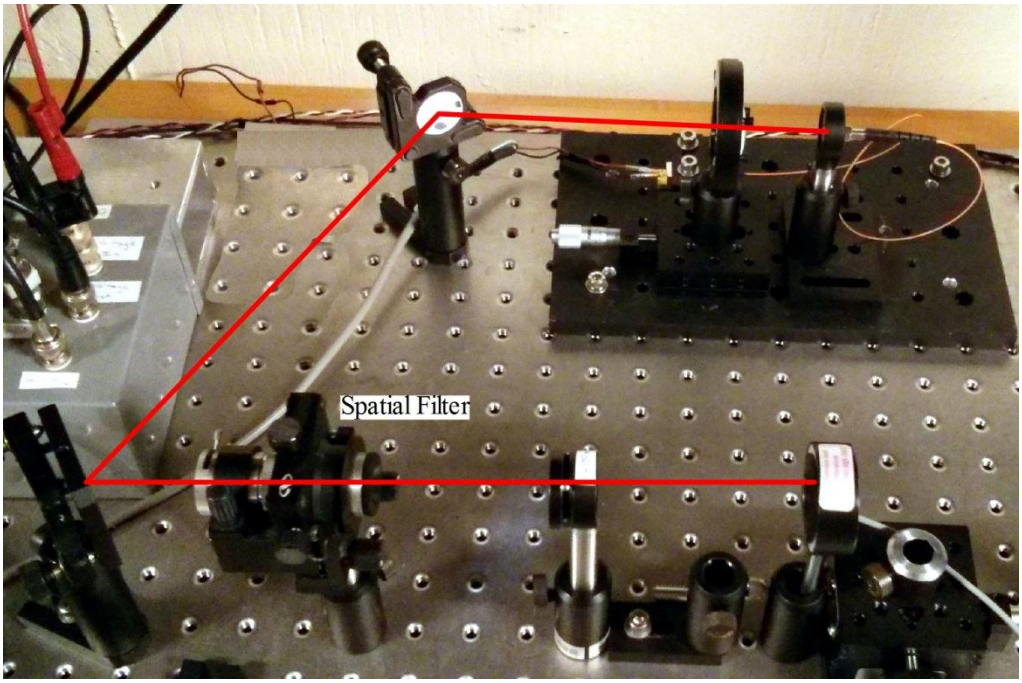

Figure 10. The setup for a spatial filter filtration of the beam.

The idea behind filtration is as follows: when the beam is focused, the Gaussian component of the beam would focus into a tight spot, while the noise would produce a pattern around the focal point. This pattern is a two-dimensional Fourier transform of the initial intensity distribution. By physically blocking everything but the spot in the middle, we can block all the imperfections and be left only with the Gaussian component of the beam. We first attempted to filter the beam with a single mode optical fiber. The entrance to the fiber is on the scale of 10's of microns, so it is very challenging to align an invisible beam to go into the fiber perfectly. In order to see the process better, we had to first send a bright red HeNe laser through the fiber from one side and align the output from the other side with the beam produced by the invisible IR diode laser. When everything was aligned perfectly, we disconnected the HeNe laser from the system and measured the power of the exiting beam. The highest throughput efficiency we could achieve was roughly 2%.

We decided to test the results by using a spatial filter, which consists of an objective that focuses the beam onto a pinhole. The overall theory behind filtration is the same as for the single mode fiber method, but the setup is easier to align and is more reliable. After adjusting the beam such that it goes into the objective's center perpendicularly and adjusting the pinhole so that it is exactly at the focal point, we were still only able to get 2% maximum throughput efficiency.

In both cases, we achieved the same throughput efficiency of 2%, which equates to 40mW on highest current, was smaller than what could be achieved with the Sanyo laser, and did not result in successful trapping. Thus, we found that it is not possible to achieve trapping by using a multimode fiber-coupled laser due to irregularity of the produced beam.

Chapter 3

Procedure

3.1 Alignment

Before we achieved any trapping of particles, we aligned the laser with the apparatus. Since laser diodes did not produce a collimated beam, we adjusted the collimating lens to produce a roughly collimated beam. We then steered the beam to hit the telescope coaxially and exactly at the center of the lens. This is important, because if the telescope is misaligned, any adjustments of the collimation would also move the beam laterally relative to the objective.

After the telescope, we had to steer the finely collimated beam trough the dichroic mirror to hit the objective coaxially and exactly at the center of the rear aperture to produce a clean focused beam exactly in the center under the front lens. When the alignment was perfect, we were able to trap particles on the slide. Figure 11 below presents a cluster of beads trapped circled in red. It can be seen that the surrounding objects (circled in blue) move, while the trapped beads remain in place.

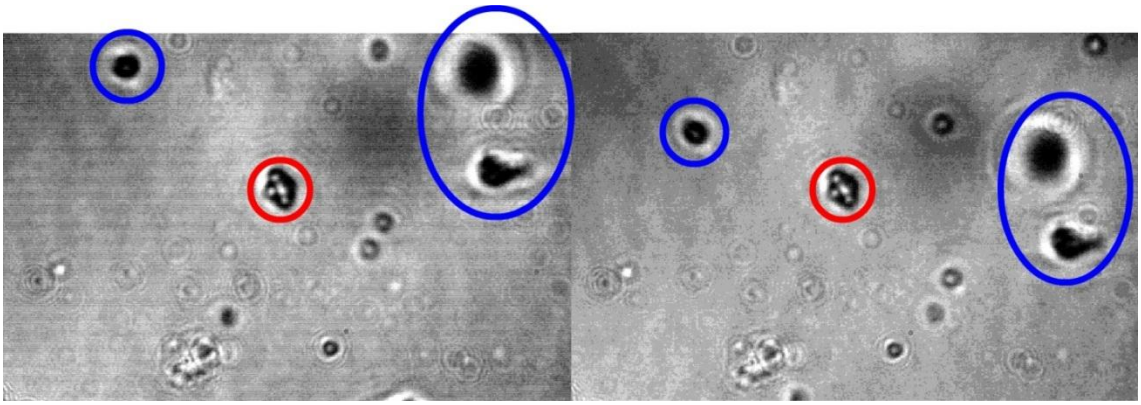

Figure 11. A cluster of beads trapped in our optical tweezers. A cluster of trapped beads circled in red remains stationary while the surroundings are moved with the stage. The most prominent surrounding artifacts (most likely dust) are circled in blue.

3.2 Trap Force Measurement

Once we were able to trap the particles, we used a LabVIEW program in order to move the piezoelectric stage at increasing speeds while keeping the trapped particle stationary, thus applying increasing drag forces due to the medium on the particle. When the drag force exceeded the force of the trap, the particle fell out of the trap. If the medium stayed stationary relative to the slide and the stage, the speed of the stage would yield a direct measurement of the drag force. There were, however, often currents present in the slide due to the facts that the objective was in contact with the cover slip and the water in the sample was evaporating because of the heat due to the backlight. Because of the currents, the real speed of the particle relative to the medium was higher than the speed reported by the program. As a result, the trapped particle would sometimes fall out of the trap at a speed lower than the maximum. In those cases, the particle would break out from the trap, but if recaptured, it would continue to be held at the same – and higher – speeds. Thus, whenever the particle fell out of the trap, we

trapped it again, and increased the speed of the stage further. It is worth noting that we maintained the same speed for four repetitions before increasing it. We would do this, until the particle would continuously fall out of the trap. Then, we recorded the speed, increased the power of the laser, and repeated the experiment. We were thus able to construct a force and velocity vs. power plot for the apparatus presented in Figure 12.

3.3 LabVIEW Program

The LabVIEW program sent consecutive signals to the piezoelectric controlled with a known frequency, thus allowing the stage to move with very specific speeds. The first version of the program was able to move the stage in 3-D with predefined parametric equations. We later found that this functionality was not useful for our purposes and made it more difficult to accurately set the speed and extract useful data. We, thus, modified the program to only be able to move the stage in one dimension with increasing speeds. The final version of the program that we used generates a seesaw signal of predefined amplitude and slope and sends it to the controller. The slope would remain constant for a predefined amount of oscillations and then increase by a specified amount. In the absence of random micro-currents in the sample, this gave us the ability to pinpoint the maximum speed at which the trap could hold the bead.

Chapter 4

Results

With Sanyo DL-8141 laser design in place, we achieved trapping of 1 μm silica beads in water solution. We then indirectly measured the force of trapping by looking at the highest speed with which we can move a trapped bead through the water solution. At the moment when the bead falls out of the trap, the hydrodynamic drag force is equal to the trap force. Using equation (3), we calculated the force from the velocity of the particle. The Velocity and Force vs. Power plot is presented in Figure 11 below. There is an evident linear relationship between the power and the force of trapping. The equations of the regression of the data are

$$v = b + m * P \quad (4)$$

$$F = b + m * P \quad (5)$$

where v is the velocity of the particle relative to the medium and is measured in μm/s, P is the power of the laser and is measured in mW, F is the force of the trap and is measured in N, b is the y-intercept and m is the slope. In equation (4), b = (7±8) μm/s and m = (0.5±0.1) mW/μm. In equation (5), b = $(6\pm8*10^{-14})$ N and m = $(5\pm1)*10^{-15}$ mW/N. The uncertainties are set as two standard deviations from the regression of the data.

The error bars presented in the plot are due to the step size used for increasing velocities. It can be seen that the step size was not the most significant uncertainty. The major source of uncertainty is the presence of the micro-currents discussed in the discussion section.

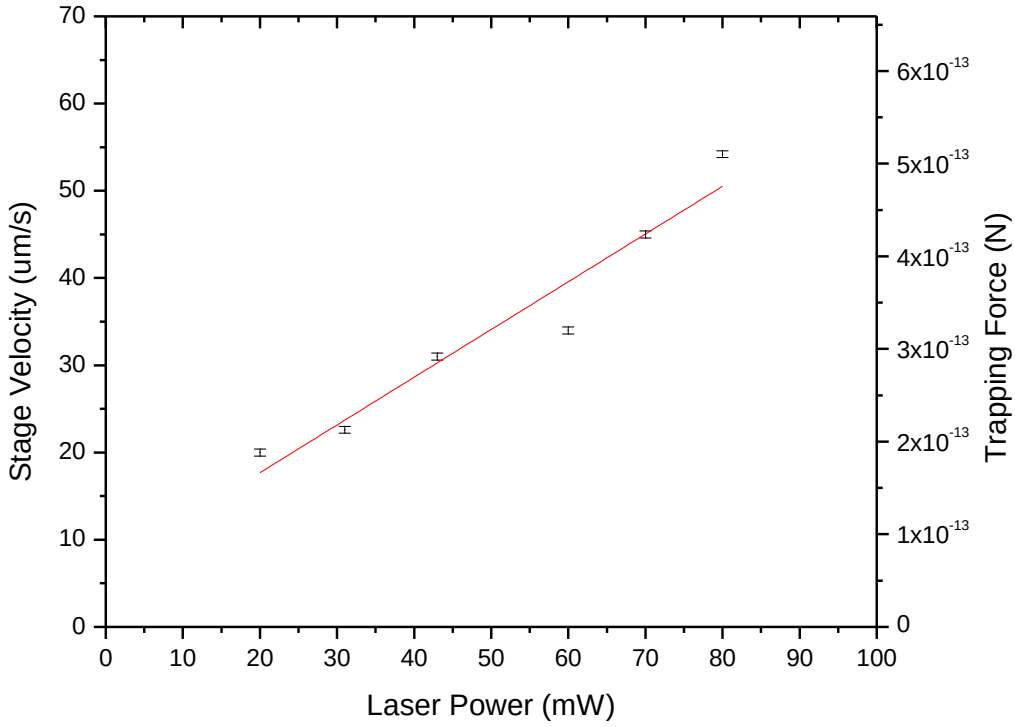

Figure 12. Velocity and Power vs. Force plot. The equation of the regression is Velocity (µm/s)= 6.73 + 0.54*Power (mW)

The major source of uncertainties in the measurement of the forces was the presence of the micro-currents that were created due to the contact of the objective with the cover slip and the evaporation of the medium due to the heat generated by the back light. There were, however, also uncertainties associated with the movement of the stage. This uncertainty arises from the fact that piezoelectrics responses exhibit hysteresis. Moreover, at the extrema the displacement per change in voltage was higher than in the middle. The displacement vs. voltage plot is presented in Figure 12 below. The regression of the data yielded the slope of 0.43 ± 0.01. If the first point were removed from the data, the slope would become 0.421±0.004. Thus, if the applied voltages were restricted to between 10 and 70 volts, the uncertainty associated with stage movement would be more than halved.

Chapter 5

Discussion

Using the setup with the Sanyo DL-8141 laser, we were able to trap and manipulate 1-micron PSS beads. We were able to determine the relationship between the power of the laser, and the force of the trap. On average, we determined that for each mW of power outputted by the laser, the trap received 5.16×10^{-15} N of force. Overall, when the laser provided power between 20 and 80 mW, the force was 2×10^{-13} to 5×10^{-13} N.

5.1 Problem of Micro-currents.

There were certain limitations to the setup that was used that contributed to the instability of the system and thus the uncertainty of the measurement of the force. The greatest cause of uncertainty was the presence of the micro-currents in the slide. These micro-currents affected the relative speed of the particle to the medium and caused the particle to escape the trap prematurely. There were two major causes for the currents: the fact that the objective was in contact with the slide; and the fact that water evaporated from the slide fairly quickly.

The problem with the objective could be solved by substituting the existing 100x objective with one of lower magnification. Since higher magnification corresponds with lower focal distances and vice versa, a 50x objective would move the focal point further from the objective and thus allow the objective to be moved further from the slide, eliminating unnecessary contact. More specifically, the cover slips that we were using (FisherBrand 12-454-100) were 0.13-0.17 mm in thickness. The objective that we were using was designed for a coverslip thickness of 0.17mm to show exactly what is under the coverslip. Thus, to achieve

trapping, the objective had to be in contact with the cover slip and even then the trapping would occur right near the cover slip. For 50x objectives, focal distances are typically double of those for 100x objective. Using a 50x objective effectively would allow us to operate further from the cover slip and at a larger range. The downside of the objective change would, however, cause the trap force at the same powers to be smaller.[11] The decrease in power is caused by the fact that the force depends on the gradient of intensity. Since lower magnification objective would move the focused point away from the objective, it would decrease the focusing angle, lead to a smaller intensity gradient, and thus decrease the trapping force.

In order to quantify the force change, let's take two objectives with identical front apertures and magnifications that differ by a factor of two. Using simple geometry, we determine that the focusing angle of the smaller magnification objective (β) relates to the focusing angle of the larger magnification objective (α) in the following way:

$$\beta = \tan^{-1}\left(\frac{1}{2} * \tan\alpha\right) \tag{6}$$

Assuming very large angles, this relationship can be approximated as:

$$\beta = 2 * \alpha \tag{7}$$

This means that if we halve magnification, we essentially double the angle and thus halve the force. Some, if not all, of the lost force, however, could be compensated for by increasing the output power of the laser.

In addition, there are 100x objectives with larger front apertures and higher working distances available on the market, but they are generally more expensive. These objectives would allow us to increase the working distance without significantly compromising the trapping force.

The problem with evaporation could be solved by creating a sealed slide. This would, however, increase the time it takes to make the slide. The application of this method would depend on the experiment. If the experiment takes a long time (more than 5 minutes) and we cannot afford to let the liquid evaporate, then it would be worthwhile to make the sealed slide. If the experiment does not take a long time (less than 5 minutes), then it would not make sense to invest more time into making a sealed slide. Also, if the experiment requires a lot of manipulation on the z-axis, the sample would have to be sealed to prevent the cover slip from moving around.

5.2 Forces Due to Change in Momentum.

Another important aspect of the measurement to consider is the force associated with the change of momentum of the particles at the point where it changes the direction of motion. If that force is comparable in magnitude to the force of drag, then it needs to be included in the calculations. In order to calculate the force of the turn, we need the mass of the particle and its acceleration at the turning point. To find the mass, we multiply the density of the polystyrene[13] (1.05 g/cm³) by the volume of a sphere with radius 0.5μm to get $5.5*10^{-16}$ kg. We also know that at the turning point, the particle undergoes acceleration of:

$$a = \frac{2v}{\Delta t} \tag{6}$$

where v is the speed of the particle and Δt the time it takes the particle to change that speed. Since speed changes abruptly, Δt is the time between the signals sent to the stage. The signals are sent at a frequency of 100 Hz, so the time between the signals is 0.01 seconds. We will perform a sample calculation for the speed of 50 microns per second, which is close to the highest speed we achieved. The acceleration would thus be:

$$a = \frac{2v}{\Delta t} = \frac{2*50*10^{-6}\frac{m}{s}}{0.01\ s} = 0.01\ \frac{m}{s^2} \quad (7)$$

Multiplying mass by the acceleration, we get the force of the turn equal to 5.5 * 10^{-18} N, which is 5 orders of magnitude lower than the forces we are observing. Thus, in order to observe a significant effect of the force of turn, we need to move the particles at speeds much higher than the stage would allow.

5.3 Importance of Collimation.

Another aspect to consider is the importance of collimation. More specifically, we need to know how accurate the position of the second collimation lens needs to be in order for the trapping distance to be near the viewing plane. Practically, it is not extremely important that the trapping distance is exactly the same as the focal distance of the objective, because all objectives have a depth of field which allows them to see certain a certain range around the focal distance. The depth of field can be calculated with the following expression:

$$DoF = \frac{\lambda*n}{NA^2} + \frac{n}{M*NA}e \quad (8)$$

where λ is the wavelength of illuminating light (in our case 570nm), n is the refractive index of the medium (1.0 for air), NA is the numerical aperture (in our case 1.25), e is the smallest sized object that can be resolved (in our case 1μm), and M is the magnification of the objective (in our case 100). Thus, the depth of field for our application is 0.37 μm. That means that at any point, we can see and distinguish individual micron-sized beads at $\frac{0.37}{2} = 0.185$ μm around the viewing point. In other words, as long as the trapping position is within that region, we will be able to see and distinguish individual beads.

The not-to-scale ray diagram of the telescope and the objective is presented in Figure 13 below. We can relate the focal distance of the objective (s_{i2}) to the distance between the second lens in the telescope (the collimation lens) and the focal point within the telescope (s_{01}).

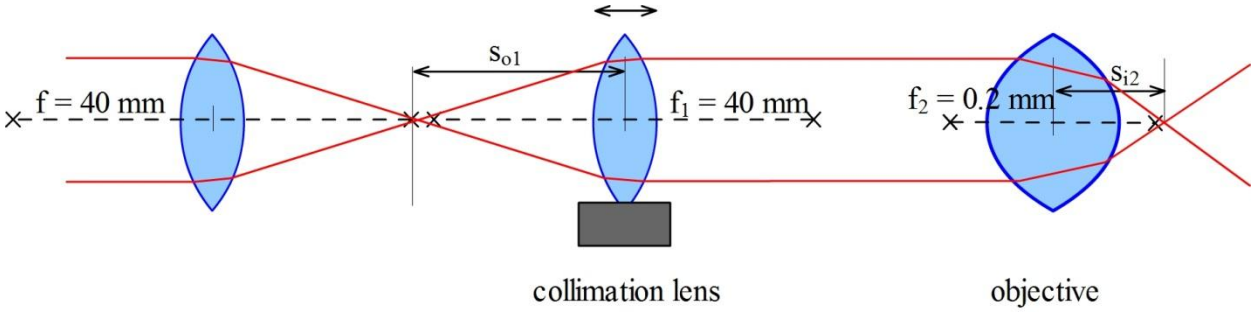

Figure 13. The not-to-scale ray diagram for the telescope and the objective.

We simplify the situation by assuming that the first lens is stationary and it produces an image at its focal length. We then relate s_{i2} and s_{o1} via an equation for two lenses below

$$s_{i2} = \frac{f_2 * d - f_2 s_{o1} f_1/(s_{o1} - f_1)}{d - f_2 - s_{o1} f_1/(s_{o1} - f_1)}$$

where f_1 is the focal length of the second lens in the telescope (40 mm); s_{o1} is the distance between the collimation lens and the focal point within the telescope (independent variable); s_{i2} is the distance between the objective and the trapping point (dependent variable); f_2 is the focal length of the objective (0.2 mm) and *d* is the distance between the objective and the collimation lens (1 m). We plotted s_{i2} vs. s_{o1} to determine how the variation of the trapping point depends on the position of the collimation lens. The plot is presented in figure 14 below.

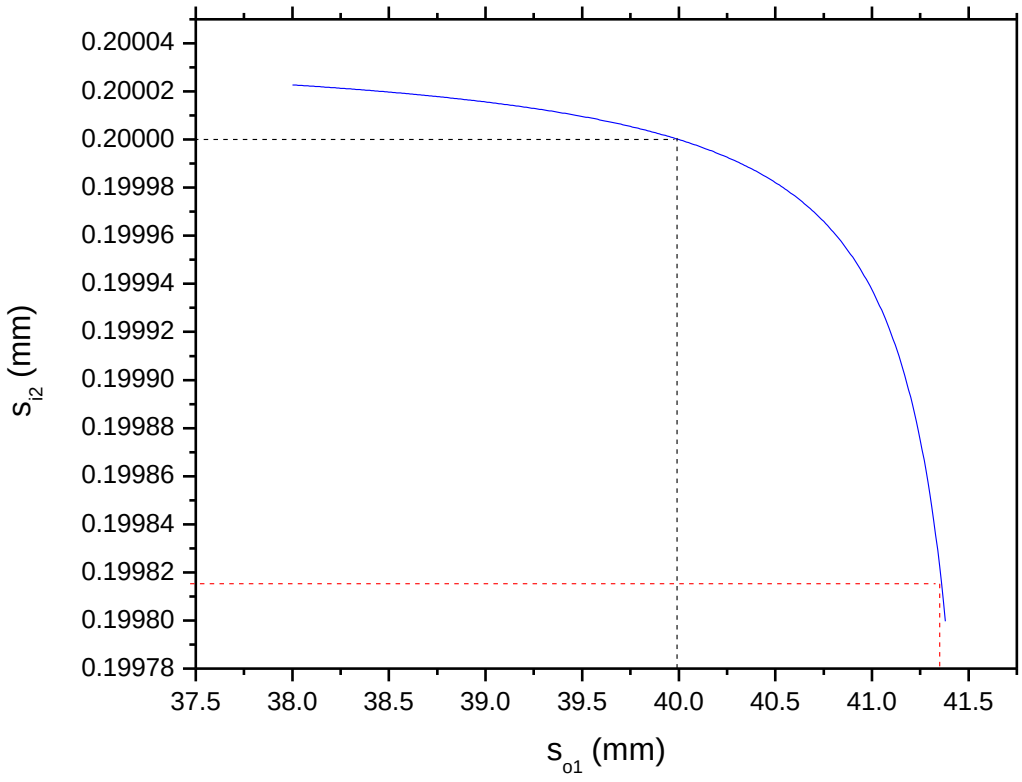

Figure 14. Distance of the trapping point from the objective vs. distance of the collimation lens from the focal point within the telescope.

We can see from the plot that when the focused point of the beam is in the focal point of the lens, the objective focuses the beam at its focal point (0.2 mm), as expected. Decreasing the distance between the collimation lens and the focus point slightly moves the trapping point away from the objective. Increasing the distance between the collimation lens and the focus point, however, asymptotically moves the trapping point towards the objective. Previously, we calculated that we can see micron-sized objects 0.185 µm (or 0.000185 mm) away from the focal distance. That means that as long as the bead is between 0.199815 mm and 0.200185 mm, we will be able to see the particle. We can see from the plot that moving the collimation lens

closer to the focus point, even by relatively large distances, will not cause major viewing problems. Moving the collimation lens away from the focus point by more than 41.3 mm, however, will move the trapping distance out of the field of view and prevent us from seeing it.

5.4 Future work

Some experiments might require manipulation of two particles. In that case, we would need to enhance the apparatus to introduce a second beam. There are a few methods that have been successfully implemented by other labs. Some of the most prominent methods involve: adding a second laser[14]; using a polarizing beam-splitting cubes[15]; and using an acousto-optic modulator[16]. Adding a second beam would allow us to study such things as interactions of cells and viruses or spring-like forces of DNA.

In a second laser setup, the second laser is added from the other side of the slide. It relies on the same concepts as a one-laser set-up but adds bulk and makes focusing, viewing, and manipulating the particles increasingly difficult.

In a polarizing beam-splitting cubes setup, polarizing beam-splitter cubes split the beam based on polarization, creating two beams that can be controlled separately and then rejoined before entering the objective. This method requires precise electrical control of the mirrors in order to steer the beams, which can be relatively expensive.

An acousto-optic setup modulator setup relies on sound waves to diffract a part of the beam. It thus produces a second beam, whose intensity and position are controlled by the intensity and frequency of the sound wave. Integrating this method into the system would require the least amount of redesign, as the secondary beam would be nearly parallel to the first one.

Bibliography

[1] C. Neuman and M. Block, Rev. Sci. Instrum. **75**, 2787 (2004);

[2] A. Ashkin, Phys. Rev. Lett. **24**, 156 (1970).

[3] A. Ashkin and J. M. Dziedzic, Appl. Phys. Lett. **19**, 283 (1971).

[4] A. Ashkin *et al.*, Opt. Lett. **11**, 288 (1986).

[5] 4 A. Ashkin, IEEE J. Sel. Top. Quantum Electron. **6**, 841 (2000).

[6] A. Ashkin, J. M. Dziedzic, and T. Yamane, Nature (London) **330**, 769 (1987).

[7] S. C. Kuo, Traffic **2**, 757 (2001).

[8] Crocker, J. C., Matteo, J. A., Dinsmore, A. D., and Yodh, A. G. Phys. Rev. Lett. **82**, 4352–4355 (1999).

[9] C. Bustamante *et al.*, Curr. Opin. Struct. Biol. **10**, 279 (2000).

[10] E. J. G. Peterman *et al.*, Rev. Sci. Instrum. **74**, 3246 (2003).

[11] A. Rohrbach and E. H. Stelzer, Appl. Opt. **41**, 2494 (2002).

[12] John F. Marko, Hydrodynamic Drag, Brownian Motion and Diffusion, http://www.uic.edu/classes/phys/phys450/MARKO/N004.html.

[13] Lide, David R. *CRC Handbook of Chemistry and Physics: A Ready-reference Book of Chemical and Physical Data*. Boca Raton, FL: CRC, 1994.

[14] M. Ribezzi-Crivellari, F. Ritort, Force Spectroscopy with Dual-Trap Optical Tweezers: Molecular Stiffness Measurements and Coupled Fluctuations Analysis, Biophysical Journal, Volume 103, Issue 9, 7 November 2012, Pages 1919-1928, ISSN 0006-3495, 10.1016/j.bpj.2012.09.022.

[15] Fällman E., Axner O., "Design for fully steerable dual-trap optical tweezers," Appl. Opt. 36(10), 2107–2113 (1997). doi: 10.1364/AO.36.002107.

[16] M. D. Wang, H. Yin, R. Landick, J. Gelles and S. M. Block "Streching DNA with Optical Tweezers," Biophys. J. **72** 1335-1346 (1997).